

## Correlation between X-Ray Absorption and Chemical Potential Measurements in Lithium Intercalated Carbons

J. R. Dahn and J. N. Reimers

*Department of Physics, Simon Fraser University, Burnaby, British Columbia, Canada V6T 1W5*

T. Tiedje<sup>(a)</sup> and Y. Gao

*Department of Physics, The University of British Columbia, Vancouver, British Columbia, Canada V6W 1Z1*

A. K. Sleight

*Moli Energy (1990) Ltd., 3958 Myrtle Street, Burnaby, British Columbia, Canada V5C 4G2*

W. R. McKinnon

*Division of Microstructural Sciences, National Research Council of Canada, Ottawa, Canada K1A 0R9*

S. Cramm

*Kernforschungsanlage Jülich GmbH, Postfach 1913, D-5170 Jülich, Germany*

(Received 2 August 1991)

Using synchrotron radiation we measured the x-ray absorption (XAS) near the  $C_{1s}$  edge for powdered graphite, boron substituted graphite, and a disordered graphitic carbon. The chemical potential of Li intercalated into the same carbons has also been measured as a function of  $x$  in  $Li_xC_6$ . When Li is intercalated, the  $2s$  electron is transferred to the C host, filling the same levels as probed by XAS. In XAS, final-state energies contain a contribution from the electron-core-hole interaction which mimics the situation in Li intercalation where  $Li^+$  interacts with conduction electrons. We show that XAS results correlate well with chemical potential measurements of intercalated Li made on the same materials.

PACS numbers: 78.70.Dm, 71.20.-b, 82.45.+z, 82.60.-s

Intercalation occurs when an intercalant can lower its free energy by entering a solid and forming chemical bonds. The chemical potential  $\mu$  of an intercalated Li atom measured with respect to Li metal is the difference in Gibbs free energy of the Li atom in the two environments and hence is a measure of the bonding between the intercalant and the host. This bonding arises when the Li  $2s$  electron is transferred to unoccupied one-electron levels in the host. In the rigid-band model one assumes that the shape of the bands is unchanged by the intercalation and that one-electron levels are sequentially filled as more intercalant is added. Thus, in the dilute limit where the intercalated species do not interact, one might expect the variation of the chemical potential with intercalant concentration,  $x$ , to match the movement of the Fermi level with respect to the rigid bands. However, the conduction electrons react to the presence of the  $Li^+$  ion and move to screen it. This many-body effect changes the energies of the one-electron eigenstates and hence first-principles calculations of  $\mu(x)$  have not yet been made for any material.

A similar screening occurs in near-edge x-ray absorption (XAS) spectroscopy. Here, a photon is used to excite a core electron into an unoccupied conduction-band state. The absorption versus photon energy then is a probe of the local density of unoccupied states in the solid. However, the final-state energies for the electron are perturbed by the presence of the core hole [1]. Although the core hole is short lived, Mahan [1] has argued that its lifetime is long enough for the static screening ap-

proximation to be used to describe its effects. Although the core hole and the intercalated  $Li^+$  ion are located at different sites in the lattice, we expect the screening around each to involve electrons near the Fermi level in  $\pi$  bands. Because the screening length in graphite is several lattice spacings, the response of the electrons to each of these charged objects should be similar. Thus, the core hole mimics the effect of the  $Li^+$  ion in the intercalation experiment. A schematic diagram to show the correspondence between XAS and Li intercalation is given in Fig. 1. In this paper we examine experimentally the correspondence between the XAS and intercalation experiments and obtain new insights into the physical processes that determine the chemical potential of intercalated atoms.

Applications for graphite intercalation compounds have been proposed for many years [2-4], and now a commercial application for  $Li_xC_6$  as an electrode in advanced rechargeable batteries [5,6] is emerging. A better understanding of the variation of  $\mu$  as a function of  $x$  is also important for these applications.

Three powdered carbons which can be electrochemically intercalated with lithium were chosen for study. Crystalline synthetic graphite designated KS-44 from Lonza Corporation and petroleum needle coke designated XP from Conoco Corporation were used. Cokes are graphitic carbons with random rotations between and translations parallel to neighboring layers ("turbostratic" disorder) [7]. A natural synthetic graphite substitutionally doped with 2.5-at.% boron using the methods of Lowell [8] (No.

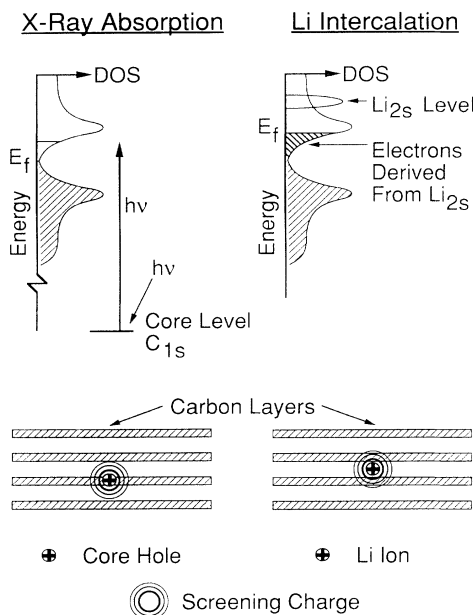


FIG. 1. Schematic diagram showing the relation between Li intercalation and x-ray absorption in carbon samples.

4900 graphite doped with 2.5% boron from Superior Graphite) was also used.  $\text{Li}/\text{Li}_x\text{C}_6$  electrochemical cells were constructed and tested as described elsewhere [9,10]. The voltage  $V$  of these cells is given by  $V = -\mu/e$ , where  $e$  is the magnitude of the electron charge [11].

Figure 2 shows  $V(x)$  for  $\text{Li}/\text{Li}_x\text{C}_6$  cells containing each of the three carbons. Both petroleum coke and the boron substituted graphite show significant regions at low  $x$  where Li atoms are more tightly bound (the cell voltage is higher) than in graphite. The composition limit,  $x=1$ , for Li intercalated graphite is caused by the filling of all possible crystallographic sites in the interlayer spaces, *not* by a filling of the available electronic states [12]. At small  $x$ , electronic screening and wide separation ensure that the Li atoms do not interact strongly with one another and it is here that we expect agreement with the XAS results to be best. At higher concentrations, Li-Li interactions lead to the well-known staged phases in graphite and in boron doped graphite [2,3] which are suppressed by the disorder in coke [9].

Figure 3 shows XAS spectra collected for the three unintercalated carbon samples measured using a total electron yield detector at beam line U1 at National Synchrotron Light Source. The estimated experimental resolution is about 0.35 eV [13]. The details of the beam line have been published elsewhere [13]. The carbon powders were pressed onto the surface of indium foils and the three samples were mounted together on a copper holder. The powders are substantially oriented after pressing so we took care to measure the absorption at the same angle of incidence ( $45^\circ$ ) for all three. This is because transitions to unfilled  $\pi$  bands in graphite depend strongly on

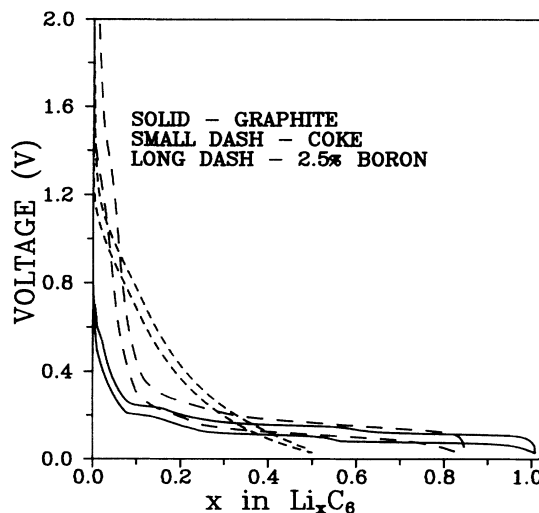


FIG. 2. Voltage vs  $x$  for  $\text{Li}/\text{Li}_x\text{C}_6$  cells measured during constant current discharge and charge. For each sample, the lower curve was measured as the lithium was intercalated (discharge) and the upper curve while the lithium was deintercalated (charge). The offset between charge and discharge is due to the “ $IR$ ” drop in the internal resistance of the cell.

the incident angle of the electric field vector to the graphite basal planes [14]. To obtain reliable XAS spectra of the carbon  $K$  edge, one must accurately measure the variation of the synchrotron beam intensity  $I_0$  with photon energy because carbon contamination of the beam-line optics leads to intensity variations in the region of interest. We made three independent measurements of the  $I_0$  variation: (1) the current flow from a gold grid placed in the beam prior to the sample, (2) the signal from a channel-plate detector placed opposite to the last mirror

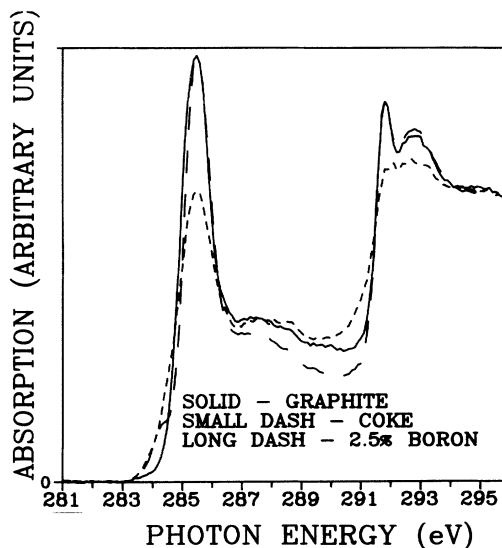


FIG. 3. X-ray absorption vs photon energy for graphite, petroleum coke, and graphite doped with 2.5-at. % boron.

in the beam-line path prior to the sample, and (3) the absorption from a freshly sputtered gold sample. The first two measurements were made during the carbon measurement and the third was done independently. The data in Fig. 3 are the electron yield from the carbon divided by the  $I_0$  signal from the channel plate [(2) above]. Using the other  $I_0$  signals gave identical results. The data for the three samples have been scaled to give the same absorption at 281 eV and at 297 eV. The data for graphite agree well with previous measurements [15], although they do not show strong evidence for the peak at 289 eV recently associated with graphite interlayer states [14]. We interpret the absorption in terms of the density of empty states above the Fermi level [16]. For example, the large peak near 286 eV, observed in previous measurements [14,15], arises from transitions to the peak in the  $\pi$ -band density of states about 2 eV above the Fermi level.

The number of sites available for intercalated Li atoms per unit chemical potential interval is proportional to the derivative  $-dx/dV$ . Therefore,  $-dx/dV$  as a function of  $V$  can be thought of as a "density of sites" per unit energy for Li. Since each intercalated Li atom transfers an electron to the carbon host, the energy to intercalate a Li atom is determined by the energy of the Li ions, the energy of the donated electrons, and the energy of interaction between the ions and the electrons. At small  $x$ , the interactions between the ions should be unimportant, so the ionic energy should be approximately constant. Then the density of sites is determined by the changes in the other two energies. Hence  $-dx/dV$  should be proportional to the density of states for electrons, taking into account the interactions of the electrons with the compensating positive charges. This is just what XAS measures; the only difference is that the compensating positive charge in XAS is in the core of the carbon atom instead of between the layers as Fig. 1 indicates. If this change in location of the positive charge does not strongly influence the screening energy, then a plot of  $-dx/dV$  vs  $\mu$  should resemble the XAS spectrum. The photon energy in the XAS spectrum plays the role of the chemical potential in the electrochemical experiment.

Figure 4 compares  $-dx/dV$  vs  $\mu$  to the XAS spectra for the three samples. To make a meaningful comparison, we have convoluted the electrochemical data (resolution of 0.005 eV [10]) with a 0.35-eV Gaussian to match the resolution of the XAS experiment. The data show remarkable agreement, especially at low photon energies and chemical potentials which corresponds to small  $x$  in  $\text{Li}_x\text{C}_6$ . The Fermi level moves by roughly 1.3 eV in graphite as Li is intercalated to the composition limit [17,18] so we expect the area of agreement between the XAS and electrochemical experiments to be within a volt or so of the edge. In boron doped graphite, there are valence-band holes [19] which must first be filled by the transferred electrons as Li is added. The effect of these

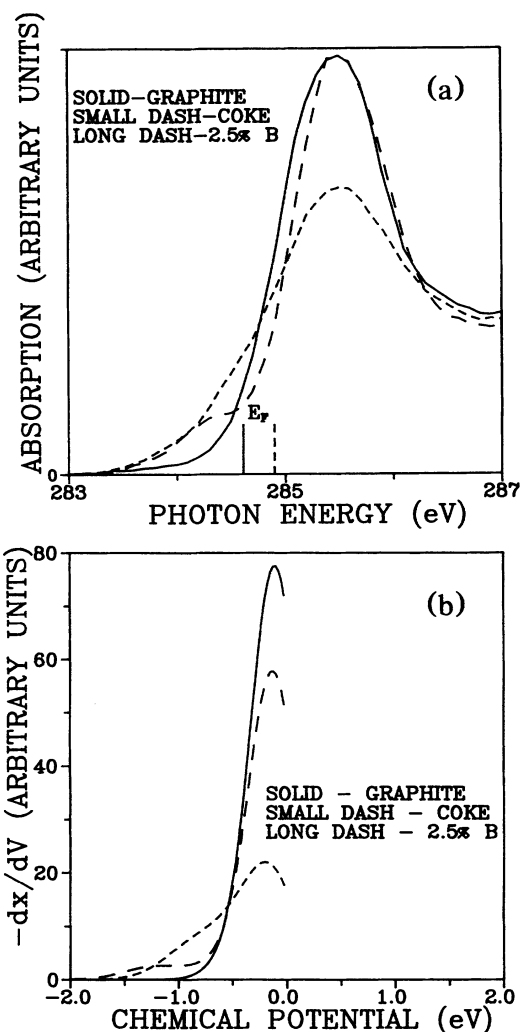


FIG. 4. Comparison of (a) x-ray absorption as a function of photon energy with (b)  $-dx/dV$  as a function of Li chemical potential. Solid and dashed lines have been used to connect the data points which were measured every 0.1 eV in (a) and every 0.005 eV in (b).

holes is clearly seen as the "foot" at low energy in both the XAS data and the electrochemical data. Petroleum coke also has sites available for electrons at higher binding energies than graphite does, as both the XAS and electrochemical results show. These states must result from the disorder in the petroleum coke, but we cannot distinguish whether they arise from differences in the one-electron density of states or differences in screening. We emphasize that the phase transitions between staged phases which form during the intercalation of Li in graphite and in the boron doped graphite are easily observed as plateaus in  $\mu(x)$  and sharp peaks in  $-dx/dV$  vs  $\mu$  [9,10]. These features have been broadened into a single peak near  $\mu = -0.2$  eV in Fig. 4 by the convolution with the Gaussian.

From photoelectron spectroscopy measurements of the  $C_{1s}$  core level, we determined that the  $C_{1s}$  binding energies for coke and graphite were 284.9 and 284.6 eV in good agreement with previous work [20]. This allows us to locate the Fermi-level positions in the XAS spectra in the absence of a core hole, as shown in Fig. 4. The small shift (0.3 eV) in the Fermi levels is presumably caused by structural differences in the materials. The nonzero absorption below the Fermi level gives an indication of the electron-core-hole correlation energy (about 1eV). The XAS spectra in Fig. 4 could be shifted so the Fermi levels align, but our conclusions are not affected.

To summarize, the interaction between an intercalated Li ion in graphite and its donated electron is very similar to the interaction between the core hole and an electron photoexcited at the threshold of the carbon  $K$  edge. The similarity between the basic physics of these two effects allows a connection between two superficially unrelated phenomena; electrochemical measurements of the chemical potential of intercalated Li and x-ray absorption spectra. This provides a new method for understanding the basic interactions involved in intercalation processes.

Some of this work was carried out at the National Synchrotron Light Source, a U.S. Department of Energy Facility. Funding was provided by the Natural Sciences and Engineering Research Council of Canada and the Simon Fraser University Presidents Fund.

<sup>(a)</sup>Also at Department of Electrical Engineering.

- [1] G. D. Mahan, *Solid State Physics*, edited by H. Ehrenreich and D. Turnbull (Academic, New York, 1974), Vol. 29, p. 76.
- [2] M. S. Dresselhaus and G. Dresselhaus, *Adv. Phys.* **30**, 139 (1981).
- [3] S. A. Solin, *Adv. Chem. Phys.* **49**, 455 (1982).
- [4] S. Basu, U. S. Patent No. 4,423,125, 27 Dec. 1983.
- [5] J. R. Dahn, U. Von Sacken, M. W. Juzkow, and H. Al-Janaby, *J. Electrochem. Soc.* **138**, 2207 (1991).
- [6] J. M. Tarascon and D. Guyomard, *J. Electrochem. Soc.* (to be published).
- [7] W. Ruland, *Acta Crystallogr.* **18**, 992 (1965).
- [8] C. E. Lowell, *J. Am. Ceram. Soc.* **50**, 142 (1967).
- [9] J. R. Dahn, Rosamaria Fong, and M. J. Spoon, *Phys. Rev. B* **42**, 6424 (1990).
- [10] J. R. Dahn, *Phys. Rev. B* **44**, 9170 (1991).
- [11] W. R. McKinnon and R. R. Haering, in *Modern Aspects of Electrochemistry*, edited by R. E. White, J. O'M. Bockris, and B. E. Conway (Plenum, New York, 1983), No. 15, p. 235.
- [12] N. Kambe, M. S. Dresselhaus, G. Dresselhaus, S. Basu, A. R. McGhie, and J. E. Fischer, *Mater. Sci. Eng.* **40**, 1 (1979).
- [13] M. Sansone, R. Hewitt, W. Eberhardt, and D. Sondericker, *Nucl. Instrum. Methods Phys. Res., Sect. A* **266**, 422 (1988).
- [14] D. A. Fischer, R. M. Wentzcovitch, R. G. Carr, A. Continenza, and A. J. Freeman, *Phys. Rev. B* **44**, 1427 (1991).
- [15] Th. Fauster, F. J. Himpsel, J. E. Fischer, and E. W. Plummer, *Phys. Rev. Lett.* **51**, 430 (1983).
- [16] N. A. W. Holzwarth, S. G. Louie, and S. Rabii, *Phys. Rev. B* **26**, 5382 (1982).
- [17] W. Eberhardt, I. T. McGovern, E. W. Plummer, and J. E. Fischer, *Phys. Rev. Lett.* **44**, 200 (1980).
- [18] N. A. W. Holzwarth, S. Rabii, and L. A. Girifalco, *Phys. Rev. B* **18**, 5190 (1978).
- [19] S. Marinkovic, in *Chemistry and Physics of Carbon*, edited by Peter A. Thrower (Marcel Dekker, New York, 1984), Vol. 19.
- [20] F. R. McFeely, S. P. Kowalczyk, L. Ley, R. G. Cavell, R. A. Pollack, and D. A. Shirley, *Phys. Rev. B* **9**, 5268 (1974).